Eur. Phys. J. B **45**, 231–235 (2005)
DOI: 10.1140/epjb/e2005-00175-6

THE EUROPEAN PHYSICAL JOURNAL B

The orientation-effect of exchange bias on giant magnetoimpedance in surface crystallized $Co_{66}Fe_4B_{15}Si_{15}$ amorphous ribbons

S.S. Yoon[1], N.A. Buznikov[2,3], D.Y. Kim[2], C.O. Kim[2], and C.G. Kim[1,a]

[1] Department of Physics, Andong National University, Andong 760-749, Korea
[2] Department of Materials Engineering, ReCAMM, Chungnam National University, Daejeon 305-764, Korea
[3] Institute for Theoretical and Applied Electrodynamics, Russian Academy of Sciences, Moscow 125412, Russia

Received 14 September 2004 / Received in final form 24 February 2005
Published online 28 June 2005 –

Abstract. A phenomenological model to describe the transverse differential susceptibility in the field-annealed CoFeBSi amorphous ribbon is developed. The exchange bias between surface crystalline layer and amorphous bulk is described by means of an exchange bias field. The model allows one to calculate the external field dependence of the transverse differential susceptibility. It is shown that so-called valve at low frequencies and asymmetric two- peak behavior at high frequencies appear in the transverse susceptibility if the orientation of the exchange bias deviates from the ribbon axis. The calculated results are in a qualitative agreement with the magnetoimpedance profiles observed in experiments and allow one to conclude that the exchange interaction between the surface crystalline layer and amorphous bulk is antiferromagnetic coupling.

PACS. 75.50.Kj Amorphous and quasicrystalline magnetic materials – 75.30.Et Exchange and superexchange interactions

1 Introduction

Exchange bias (EB) is one of the phenomena associated with the unidirectional magnetic anisotropy created at an interface between a ferromagnetic and an antiferromagnetic material [1]. The EB has attracted extensive interest in research because of its potential applications in magnetoresistive (MR) heads and sensors, where the EB makes asymmetric MR effect with respect to the applied magnetic field [2–5].

The giant magnetoimpedance (MI) effect consists of huge changes in the complex impedance of soft magnetic materials upon application of an external magnetic field. Since the MI sensor, magnetic sensor based on the MI effect, has 10,000 times the sensitivity of the MR sensors and can be very promising for a new generation of sensor devices, much attention has been paid recently to the MI effect [6,7]. To build MI sensor, asymmetric MI element are needed. Asymmetric characteristics have been produced by applying dc current or ac bias field on symmetric MI elements [8,9].

The asymmetric MI characteristics created by the EB have been first reported by Kim et al. in 1999 [10], when CoFeBSi ribbons have been annealed in air at 380 °C in the presence of a weak magnetic field about 3 Oe applied along the ribbon. Because the ribbons annealed in vacuum did not show the asymmetric MI characteristics, oxidation plays important role in the phenomena. It has been confirmed by the X-ray diffraction spectra using the grazing incidence diffraction method that the crystalline layer containing hcp-Co and fcc-Co crystallites is developed on the surface of the ribbon annealed in air at 380 °C [11]. The composition-depth profile measured by Auger electron spectroscopy has shown that B-depleted layer is developed between oxidation layer and amorphous bulk due to the diffusion of B to the surface to form oxidation. The differential thermal analysis profile of the ribbon annealed in air has shown that B-depleted layer has crystallization temperature about 330 °C, much lower than the crystallization temperature of the amorphous bulk about 540 °C [12]. It has been suggested that the exchange interaction between the surface crystalline layer and amorphous bulk produces unidirectional anisotropy, which is responsible for the asymmetric MI [13,14].

In this paper, we propose a model to describe the transverse differential susceptibility in the field-annealed amorphous ribbon by considering the EB between surface

[a] e-mail: cgkim@cnu.ac.kr

crystalline layer and amorphous bulk. The model proposed allows one to predict the field dependence of the transverse susceptibility and to explain that the origin of the asymmetric MI is the orientation of the EB.

2 Model

The Co based ribbons field-annealed in air have layered structure of crystallines/amorphous bulk. In order to develop the model to describe the magnetization variation in amorphous bulk under the influence of ac current and external magnetic field applied along the ribbon, we assume a simplified domain structure in amorphous bulk, which consists of antiparallel domains with width d in a demagnetized state as shown in Figure 1a. Figure 1b presents a schematic diagram of the angles involved in the model, where H is the external field, h is the transverse ac field induced by the ac current and H_{an} is the annealing field. It is assumed that the amorphous bulk has the uniaxial anisotropy constant K, and the anisotropy axis makes the constant angle θ_k with the longitudinal direction. We assume also that the effective bias field H_{ex} acts on the amorphous bulk with the constant angle θ_{ex} due to the unidirectional exchange anisotropy. If the amorphous bulk interacts ferromagnetically or antiferromagnetically with the crystalline layer, H_{ex} is parallel or antiparallel to the direction of the effective magnetization M_c in the crystalline layer.

Because the hysteresis loops of the as-cast and annealed ribbons have shown that the coercivity H_c of the amorphous bulk and surface crystalline layer are about 15 Oe and 150 Oe, respectively [15], the direction of M_c does not change within a relatively wide range of the external magnetic field. The domain-wall displacement x and the magnetization angles ϕ_1 and ϕ_2 can be found by the usual method of the free energy minimization [16]. Neglecting the magnetostatic energy, the free energy density U of the amorphous bulk can be written as

$$U = U_a + U_H + U_h + U_{ex} + U_w, \tag{1}$$

where U_a is the uniaxial anisotropy energy, U_H is the Zeeman energy for H, U_h is the Zeeman energy for h, U_{ex} is the unidirectional anisotropy energy by the exchange interaction and U_w is the domain-wall energy. These energy terms are given by

$$U_a = K\left[\alpha \sin^2(\theta_k - \phi_1) + (1-\alpha)\sin^2(\theta_k - \phi_2)\right] \tag{2a}$$

$$U_H = -\mu_0 M_s H\left[\alpha\cos\phi_1 + (1-\alpha)\cos\phi_2\right] \tag{2b}$$

$$U_h = -\mu_0 M_s h\left[\alpha\sin\phi_1 + (1-\alpha)\sin\phi_2\right] \tag{2c}$$

$$U_{ex} = -\mu_0 M_s H_{ex}\left[\alpha\cos(\theta_{ex} - \phi_1) + (1-\alpha)\cos(\theta_{ex} - \phi_2)\right] \tag{2d}$$

$$U_w = Awx^2 \sin^2\theta_k, \tag{2e}$$

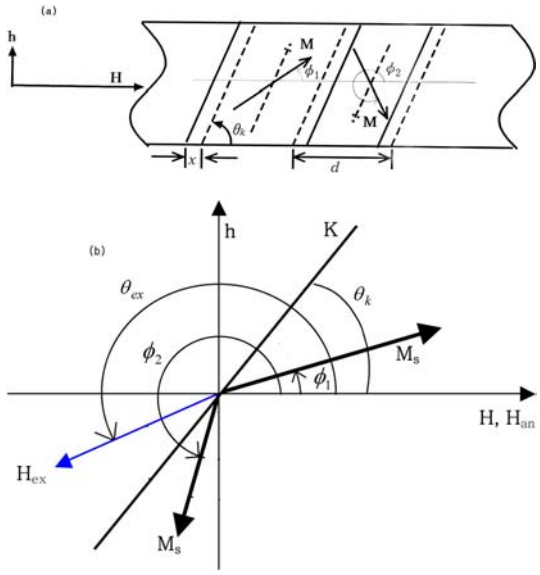

Fig. 1. Schematic diagram of domain structure and angles used in the model.

where μ_0 is the permeability of free space, M_s is the saturation magnetization and α is the volume fraction of the domain with the equilibrium magnetization angle ϕ_1, which is given by

$$\alpha = 1/2 + x/d. \tag{3}$$

The domain-wall energy is represented in equation (2e) by a parabolic potential, in which w is a measure of the wall stiffness and A is the wall area per unit volume. The equilibrium magnetization angles in domains can be found from the condition $\partial U/\partial\phi_1 = \partial U/\partial\phi_2 = 0$, which results in the following equation:

$$-\sin 2(\theta_k - \phi_i) + 2(H/H_a)\sin\phi_i - 2(h/H_a)\cos\phi_i - 2(H_{ex}/H_a)\sin(\theta_{ex} - \phi_i) = 0, \tag{4}$$

where i =1, 2 and $H_a = 2K/\mu_0 M_s$ is the anisotropy field. Equation (4) has two different solutions corresponding to the free energy minimum condition, $\partial^2 U/\partial{\phi_i}^2 > 0$, within some range of the external magnetic field. It is assumed that the domain structure in the amorphous bulk appears to minimize the magnetostatic energy, when equation (4) gives two different solutions. When equation (4) has a single solution for some external magnetic field, the structure becomes the single-domain.

The equilibrium domain-wall displacement x is given by the relation $\partial U/\partial x = 0$, which leads to equation:

$$\beta(x/d) = -\sin^2(\theta_k - \phi_1) + \sin^2(\theta_k - \phi_2) + 2(H/H_a)(\cos\phi_1 - \cos\phi_2) + 2(h/H_a)(\sin\phi_1 - \sin\phi_2) + 2(H_{ex}/H_a)\left[\cos(\theta_{ex} - \phi_1) - \cos(\theta_{ex} - \phi_2)\right], \tag{5}$$

where ϕ_1 and ϕ_2 are the solutions of equation (4), and dimensionless domain-wall parameter β is defined by the relation:

$$\beta = \frac{2Awd^2 \sin^2 \theta_k}{K}. \quad (6)$$

When we obtain the equilibrium angles ϕ_1 and ϕ_2 by equation (4) and the domain-wall displacement x by equation (5), the transverse magnetization M_t can be found as a function of H and h from the following equation:

$$M_t(H,h)/M_s = (1/2 + x/d)\sin\phi_1 + (1/2 - x/d)\sin\phi_2 \quad (7)$$

where ϕ_1, ϕ_2 and x are the solutions of equation (4) and equation (5) at given H and h. Then, the differential transverse susceptibility χ_t can be calculated as

$$\chi_t(H) = \lim_{h\to 0} \frac{M_t(H,h) - M_t(H,h=0)}{h}. \quad (8)$$

The susceptibility χ_t obtained by means of equation (8) holds only at low frequencies, when the magnetization rotation and the domain-wall displacement oscillate without phase delay with the small ac field h. At high frequencies, the domain walls are damped by eddy currents, and the susceptibility is determined by the magnetization rotation only. In this case, the dependence $\chi_t(H)$ can be also found from equation (8) by putting $x(H,h) = x(H,h=0)$, since the domain walls remain at equilibrium position without oscillation.

3 Results and discussion

Figures 2a and b show respectively the change in the equilibrium angles and the domain-wall displacement with the external dc field H calculated by means of equations (4) and (5) for $\theta_k = 70°$, $\theta_{ex} = 0°$, $H_{ex}/H_a = 0.3$, $h/H_a = 0$ and $\beta = 2$. In this case, the direction of effective magnetization M_c in the crystalline layer is parallel to the annealing field, and the amorphous bulk interacts ferromagnetically with the crystalline layer. It follows from Figures 2a and b that the domain wall exists only within the field range of $-1 < H/H_a < 0.4$. Even when the field H is absent, the magnetization angles and the domain-wall position show some rotation from the axis of the uniaxial anisotropy and some displacement from original position, respectively, due to H_{ex} as shown in the inset in Figure 2a. Figure 2c presents the transverse magnetization at the equilibrium states of Figures 2a and b. The dependence $M_t(H)$ shows a typical magnetization curve of magnetic materials with uniaxial anisotropy besides of the shift of the curve to negative H due to the presence of H_{ex}. When we apply the ac field h at equilibrium states of Figures 2a and b, the equilibrium angles and the domain-wall displacement oscillate with some amplitudes which can be calculated by equations (4) and (5). Then, the differential transverse susceptibility $\chi_t(H)$ can be calculated as a function of H by means of equation (8).

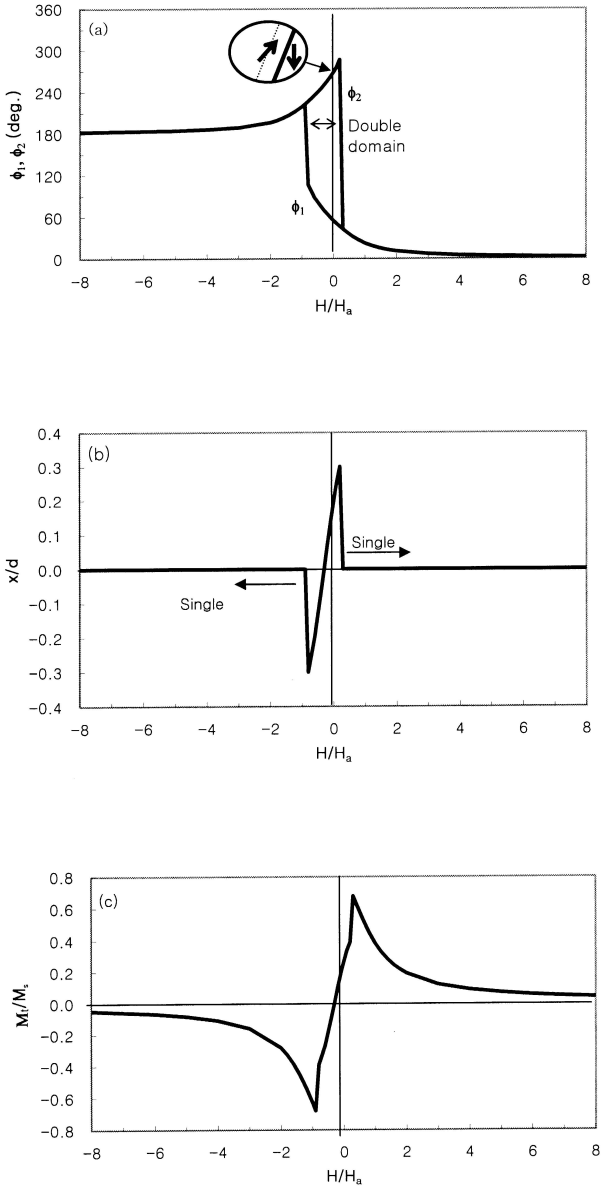

Fig. 2. The dependences of (a) equilibrium angles of magnetization, (b) domain-wall displacement and (c) transverse magnetization on external field H calculated for $\theta_k = 70°$, $\theta_{ex} = 0°$, $H_{ex}/H_a = 0.3$, $h/H_a = 0$, $\beta = 2$.

Shown in Figures 3a and b is the dependence of χ_t on H at low and high frequencies calculated by means of equation (8) for $\theta_k = 70°$, $\theta_{ex} = 0°$, $H_{ex}/H_a = 0.3$ and $\beta = 2$. At low frequency, the dependence $\chi_t(H)$ exhibits a typical single-peak behavior due to the domain-walls motion, and at high frequency, the dependence shows two peaks determined by the magnetization rotation. It follows from Figure 3 that the presence of the EB field with $\theta_{ex} = 0°$ results in only a shift of the dependence $\chi_t(H)$ towards a negative value of the external field without any asymmetry.

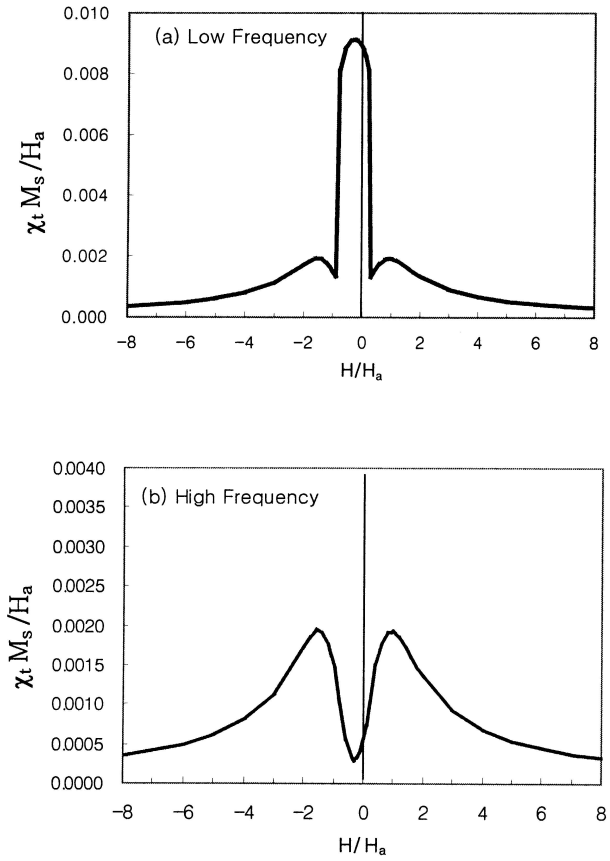

Fig. 3. The dependence of transverse susceptibility on external field H (a) at low and (b) high frequency. $\theta_k = 70°$, $\theta_{ex} = 0°$, $H_{ex}/H_a = 0.3$, $\beta = 2$. The susceptibility is normalized to make dimensionless quantity. Actually, the susceptibility was obtained by equation (8) with $h/H_a = 0.05$. However, we have confirmed that the $\chi_t(H)$ for samller h/H_a such as 0.03 and 0.01 are not very different from the curve at $h/H_a = 0.05$.

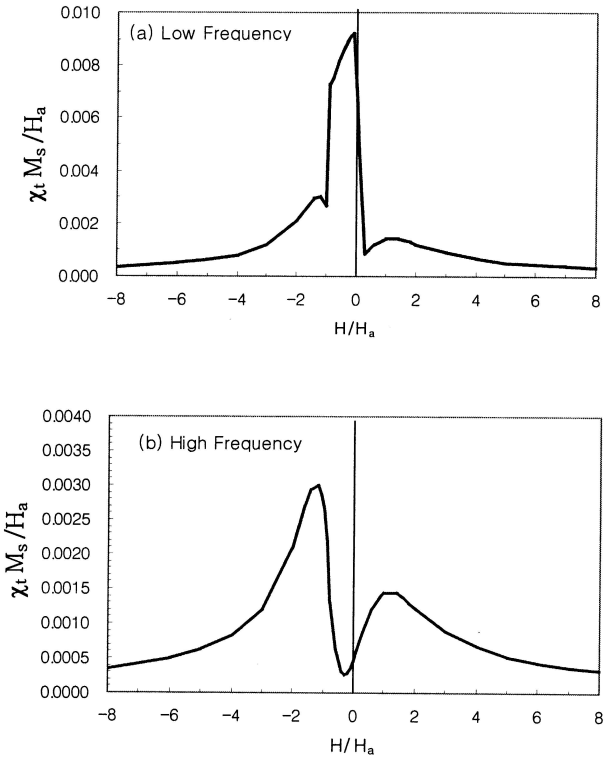

Fig. 4. The dependence of transverse susceptibility on external field H (a) at low and (b) high frequency. $\theta_k = 70°$, $\theta_{ex} = 30°$, $H_{ex}/H_a = 0.3$, $\beta = 2$.

It should be noted that it is assumed above that the effective magnetization M_c in the crystalline layer is parallel to the annealing field. However, the direction of M_c may differ from that of the annealing field due to the influence of the uniaxial anisotropy in the amorphous bulk on the crystallization process during annealing. As a result, the direction of M_c deviates from the ribbon axis and lies within the range of angles of the uniaxial anisotropy and annealing field.

The dependence of χ_t on H calculated at $\theta_{ex} = 30°$ and $\theta_{ex} = 210°$ is shown in Figures 4 and 5. The cases of $\theta_{ex} = 30°$ and $\theta_{ex} = 210°$ correspond to ferromagnetic and antiferromagnetic interaction between the amorphous bulk and surface crystalline layer, respectively, when the effective magnetization M_c in the surface layer lies within the range of angles of the uniaxial anisotropy and annealing field. It follows from Figures 4 and 5 that the valve, such as spin-valve in MR curve, at low frequency and the asymmetric two peaks at high frequency appear in $\chi_t(H)$ profiles, if the EB field deviates from the ribbon axis. When the exchange coupling is ferromagnetic, the valve lies at the negative side of H, and, at high frequency, the peak at the negative side is higher than that at the positive side (see Fig. 4). When the exchange coupling is antiferromagnetic, the reversed characteristics appear (see Fig. 5).

Since the MI is an increasing function of χ_t, the MI profile can be predicted from the calculated dependence $\chi_t(H)$. The calculated results in Figure 5 are in a qualitative agreement with the MI profiles observed in experiments, because the MI profiles shows the valve at the positive side of H at 100 kHz and the asymmetric two-peak behavior at 10 MHz where, the peak at the positive side of H is higher than that at the negative side [10,13]. Thus, the model proposed allows one to conclude that M_c lies within the range of angles of the uniaxial anisotropy and annealing field, and the exchange interaction between the crystalline layer and amorphous core is the antiferromagnetic coupling.

4 Conclusion

A phenomenological model to describe the field dependence of the transverse susceptibility in the field-annealed amorphous ribbon is developed. The effect of the surface crystalline layer on the susceptibility is described in terms of the effective bias field. It is shown that the existence of the EB is the main origin for the valve at low frequencies and the asymmetric two-peak behavior of the MI profiles

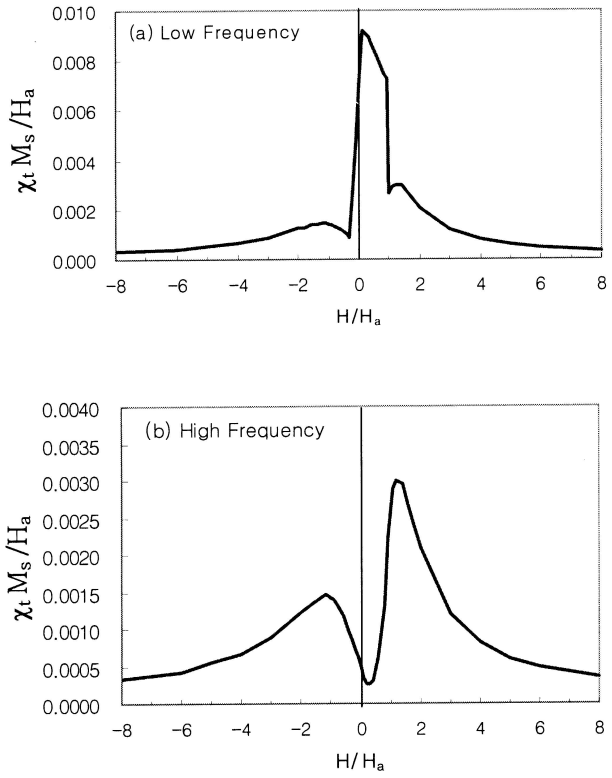

Fig. 5. The dependence of transverse susceptibility on external field H (a) at low and (b) high frequency. $\theta_k = 70°$, $\theta_{ex} = 210°$, $H_{ex}/H_a = 0.3$, $\beta = 2$.

at high frequencies observed in the experiments [10,13]. The analysis of the calculated dependences of the transverse susceptibility allows one to conclude that the effective magnetization in the crystalline layer deviates from the annealing field direction and the exchange interaction between the surface layer and amorphous bulk is antiferromagnetic coupling.

This paper was accomplished with research fund provided by Korean Council for University Education, support for 2004 Domestic Faculty Exchange. N.A. Buznikov acknowledges the support of the Brain Pool program.

References

1. J. Nogues, I.K. Schuller, J. Magn. Magn. Mater. **192**, 203 (1999)
2. R.D. Hempstead, S. Krongelb, D.A. Thomson, IEEE Trans. Magn. **14**, 521 (1978)
3. J. Fujikata, K. Ishihara, K. Hyashi, H. Yamamoto, K. Yamada, IEEE Trans. Magn. **31**, 3939 (1995)
4. T. Lin, C. Tsang, R.E. Fontana Jr., J.K. Howard, IEEE Trans. Magn. **31**, 2584 (1995)
5. B. Dieny, V.S Speriosu, S.S.P. Parkin, B.A. Gurney, D.R. Wilhoit, D. Mauri, Phys, Rev. B **43**, 1297 (1991)
6. Y. Honkura, J. Magn. Magn. Mater. **249**, 375 (2002)
7. K. Mohri, K. Kawashima, T. Kohzawa, H. Yoshida, IEEE Trans. Magn. **28**, 3150 (1992)
8. T. Kitoh, K. Mohri, T. Ushiyama, IEEE Trans. Magn. **31**, 3137 (1995)
9. D.P. Maknovskiy, L.V. Panina, D.J. Mapps, Appl. Phys. Lett. **77**, 121 (2000)
10. C.G. Kim, K.J. Jang, H.C. Kim, S.S. Yoon, J. Appl. Phys. **85**, 5447 (1999)
11. C.G. Kim, C.O. Kim, S.S. Yoon, T. Stobiecki, W. Powroznik, J. Magn. Magn. Mater. **242-245**, 467 (2002)
12. Y.W. Rheem, C.G. Kim, C.O. Kim, S.S. Yoon, J. Appl. Phys. **91**, 7433 (2002)
13. C.G. Kim, C.O. Kim, S.S. Yoon, J. Magn. Magn. Mater. **249**, 293 (2002)
14. Y.W. Rheem, L. Jin, S.S. Yoon, C.G. Kim, C.O. Kim, IEEE Trans. Magn. **39**, 3100 (2003)
15. E.E. Shalyguina, E.A. Ganshina, Y.W. Rheem, C.G. Kim, C.O. Kim, Physica B **327**, 300 (2003)
16. D. Atkinson, P.T. Squire, J. Appl. Phys. **83**, 6569 (1998)